Department of Virology, Research Institute for Microbial Diseases, Osaka University, 3-1 Yamadaoka, Suita, Osaka 565-0871, Japan

Kazuyoshi Ikuta
Department of Virology, Research Institute for Microbial Diseases, Osaka University, 3-1 Yamadaoka, Suita, Osaka 565-0871, Japan

* Corresponding author. Tel.: +81 78 599 5095; fax: +81 78 303 2561.
E-mail address: urayama-takeru@jbpo.or.jp (T. Urayama)

22 September 2012

[1] Present address: Research and Development Division, Japan Blood Products Organization, 1-5-2 Minatojima-minamimachi, Chuo-ku, Kobe-shi, Hyogo 650-0047, Japan.

Immunobiology 218 (2013) 527–532

Contents lists available at SciVerse ScienceDirect

Immunobiology

journal homepage: www.elsevier.com/locate/imbio

Jurkat cell proliferation is suppressed by *Chlamydia* (*Chlamydophila*) *pneumoniae* infection accompanied with attenuation of phosphorylation at Thr389 of host cellular p70S6K

Itaru Hirai[a,b,*], Megumi Ebara[a], Shoko Nakanishi[a], Chihiro Yamamoto[a], Tadahiro Sasaki[c], Kazuyoshi Ikuta[c], Yoshimasa Yamamoto[a,d]

[a] Department of Biomedical Informatics, Osaka University Graduate School of Medicine, Suita, Osaka 565-0871, Japan
[b] Global Collaboration Center, Osaka University, Toyonaka, Osaka 560-0043, Japan
[c] Department of Virology, Research Institute for Microbial Diseases, Osaka University, Suita, Osaka 565-0871, Japan
[d] Osaka Prefectural Institute of Public Health, Higashinari-ku, Osaka 537-0025, Japan

ARTICLE INFO

Article history:
Received 23 February 2012
Received in revised form 20 June 2012
Accepted 20 June 2012

Keywords:
Chlamydia pneumoniae
Infection
p70S6 kinase
Phosphorylation
Proliferation
T cell

ABSTRACT

Chlamydia (*Chlamydophila*) *pneumoniae* infects T lymphocytes and multiplies within them. Our previous studies have indicated that *C. pneumoniae* infection suppresses proliferation of peripheral blood mononuclear cells stimulated with *Staphylococcus*-enterotoxin B; however, the mechanism of suppression was unclear. In this study, we explored the molecular mechanism involved in *C. pneumoniae* infection by using human acute T cell leukemia cell line, Jurkat E6-1. Proliferation of Jurkat cells was suppressed in an m.o.i.-dependent manner by *C. pneumoniae* infection. The suppression by the infection was particularly evident during the initial 24 h of the infection, and down modulation of cyclin D3 protein levels were observed at the same time period by immunoblot analysis. The suppression of the Jurkat cell proliferation and the down modulation of cyclin D3 protein level were only induced by viable *C. pneumoniae* infection, not by exposure to UV-killed or heat-killed *C. pneumoniae*. Phosphorylations at Thr308 and Ser473 of AKT were induced by *C. pneumoniae* infection; however, phosphorylation at Thr389 of the downstream kinase, p70S6K was inhibited by unidentified mechanism associated with *C. pneumoniae* infection. Taking into account that G1 arrest of the *C. pneumoniae* infected Jurkat cells were not observed and that p70S6K is one of the most important regulators of protein synthesis, it was suggested that the suppression of Jurkat cell proliferation by *C. pneumoniae* was at least in part mediated by down modulation of protein synthesis through attenuation of Thr389 phosphorylation of p70S6K.

Introduction

Chlamydia (*Chlamydophila*) *pneumoniae* is an obligate intracellular bacterium. Respiratory tract *C. pneumoniae* infection is one of the major causes of community-acquired pneumonia, bronchitis, and sinusitis. Seroepidemiological and histopathological studies have detected *C. pneumoniae* antigens or the bacteria itself within atherosclerotic lesions, suggesting that *C. pneumoniae* infection may be related to the pathogenesis of atherosclerosis and cardiovascular diseases (Grayston 2000; Mussa et al. 2006; Watson and Alp 2008). Interaction between host cells and *C. pneumoniae* is thought to play a prominent role in the pathogenesis of these inflammatory diseases. However, the pathogenic mechanisms involved in the diseases associated with *C. pneumonia* infection are still unclear.

Many studies have reported the preferred host cell types for *C. pneumoniae*. *C. pneumoniae* can infect and multiply in endothelial cells, aortic smooth muscle cells, monocytes/macrophages (Gaydos et al. 1996; Godzik et al. 1995; Kalayoglu et al. 2001; Quinn and Gaydos 1999; Airenne et al. 1999), and lymphocytes (Haranaga et al. 2001a,b; Yamaguchi et al. 2002a,b). It has been hypothesized that circulating monocytes or lymphocytes infected with *C. pneumoniae* may act as carriers of the bacteria from the respiratory tract to the peripheral endothelial or smooth muscle cells, or as a reservoir of infected *C. pneumoniae* near and at the lesion in the development and progression of atherosclerosis. In

Abbreviations: PBMC, peripheral blood mononuclear cell; FCS, fetal calf serum; FITC, fluorescein isothiocyanate; LPS, lipopolysaccharide; HBSS, Hank's balanced salt solution; PI3K, mammalian target of rapamycin; mTOR, phosphoinositide 3-kinase; mTORC1, multi-component mTOR complex 1; AMPK, 5′ AMP-activated protein kinase; gadd34, growth arrest and DNA damage protein 34.

* Corresponding author at: Global Collaboration Center, Osaka University, 1-16 Machikaneyama, Toyonaka, Osaka 560-0043, Japan. Tel.: +81 6 6850 6834; fax: +81 6 6850 5185.
E-mail address: hiraii@glocol.osaka-u.ac.jp (I. Hirai).

0171-2985/$ – see front matter © 2012 Elsevier GmbH. All rights reserved.
http://dx.doi.org/10.1016/j.imbio.2012.06.008

the pathogenesis of these inflammatory diseases, lymphocytes are regarded as key contributors to acute and chronic inflammation. Therefore, investigation into how *C. pneumoniae* infection modulates the functions of lymphocytes is important for understanding the development of the inflammatory diseases associated with *C. pneumoniae* infection. We have previously reported the effects of *C. pneumoniae* infection on human peripheral blood mononuclear cells (PBMCs) (Haranaga et al. 2001a,b; Yamaguchi et al. 2008, 2004; Hirai et al. 2010) and established human T lymphocytes (Yamaguchi et al. 2002a,b; Takano et al. 2005). Recently, we reported that *C. pneumoniae* infection suppresses proliferation of *Staphylococcus*-enterotoxin B stimulated PBMCs (Hirai et al. 2010). However, the mechanism by which this occurs has not been well explained. In this study, we aimed to elucidate the effect of *C. pneumoniae* on the proliferation of T lymphocytes using Jurkat, clone E6-1 cells as an infection model. The results obtained in this study suggest that *C. pneumoniae* might exert a suppressive effect on T lymphocytes via suppression of Thr389 phosphorylation of p70S6K, which is indispensable to protein synthesis and cell proliferation.

Materials and methods

Cell lines

The human acute T cell leukemia cell line, Jurkat, clone E6-1 (Jurkat; ATCC TIB-152), and the human epithelial cell line HEp-2 (ATCC CCL-23) were obtained from the American Type Culture Collection (ATCC, Manassas, VA). Jurkat cells were maintained in RPMI 1640 medium supplemented with 10% fetal calf serum (FCS) and antibiotics (10 μg/ml gentamicin, 10 μg/ml vancomycin, and 1 μg/ml amphotericin B). HEp-2 cells were cultured in Dulbecco's modified Eagle medium supplemented with 10% FCS and the same antibiotics.

Bacteria

C. pneumoniae strain TW183 was obtained from the ATCC and propagated in HEp-2 cells according to previously described methods (Yamaguchi et al. 2002a,b). Heat-killed and UV-killed *C. pneumoniae* were prepared as described in previous reports (Hirai et al. 2010; Geng et al. 2000). The number of infectious *C. pneumoniae* cells was determined as inclusion forming units, by counting the inclusion bodies formed in *C. pneumoniae* infected HEp-2 cells after staining with fluorescein isothiocyanate (FITC)-conjugated monoclonal anti-*Chlamydia* antibody specific to *Chlamydia* lipopolysaccharide (LPS) (Denka seiken, Tokyo, Japan) (Hirai et al. 2010).

C. pneumoniae infection

Jurkat cells were seeded at 0.5 or 1.0×10^7 cells/well in a 24-well plate on the day of *C. pneumoniae* infection. *C. pneumoniae* cells were added to Jurkat cells at an m.o.i. of 0, 1, 10, 30, or 100. The plate was then centrifuged at $700 \times g$ for 60 min at room temperature. After centrifugation, the cells were washed twice with Hank's balanced salt solution (HBSS), and cultured in RPMI 1640 medium supplemented with 10% FCS and the previously itemized antibiotics. The Jurkat cells were collected at 0, 1, 2, 3, 4, 5, 8, 24, 48, and 72 h after infection and subjected to experiments. In some experiments, Jurkat cells were treated with 10 μM of cytochalasin D (Wako Pure Chemical Industries, Ltd., Osaka, Japan) since 30 min before and during the centrifugation. In some experiments, heat-killed and UV-killed *C. pneumoniae* were used. The treated Jurkat cells were collected after 0, 24, 48, and 72 h of exposure, for further analysis.

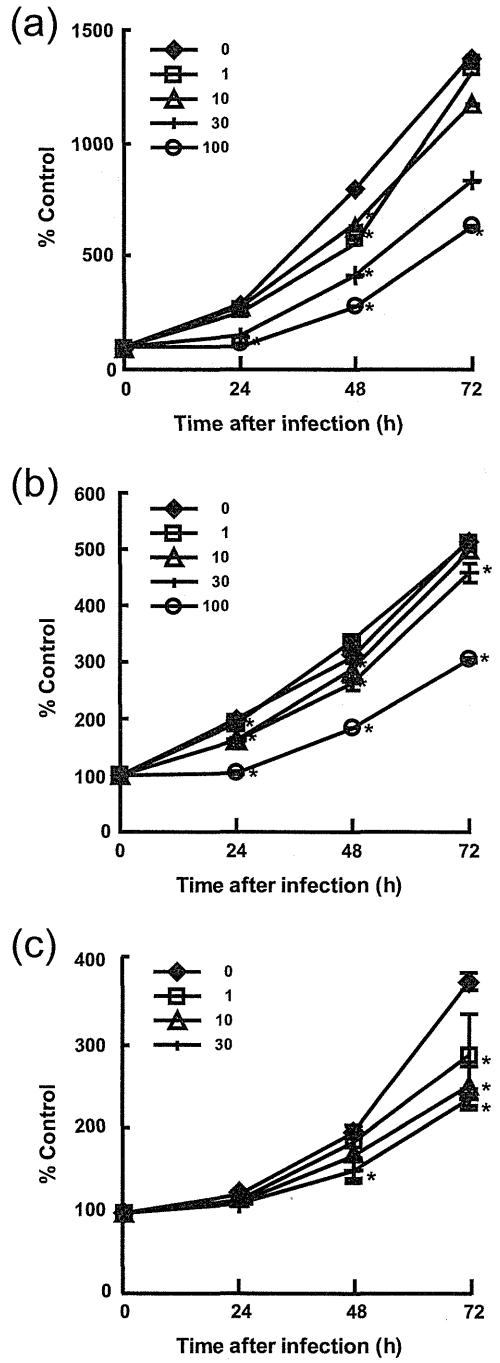

Fig. 1. Suppression of Jurkat cell proliferation by *C. pneumoniae* infection. Jurkat cells and HEp-2 cells were infected with *C. pneumoniae* at an m.o.i. of 0, 1, 10, 30 or 100 and of 1, 1, 3, 10 or 30, respectively. At 0, 24, 48, and 72 h after infection, cells were collected. The relative viable cell ratios of the infected Jurkat cells (a), and the relative viabilities of the infected Jurkat cells (b) and the infected HEp-2 cells (c) were measured. Representative results from 3 independent experiments are shown. The numbers indicate the value relative to the control group at time point 0, and are represented as means ± standard deviations ($n = 3$). *$P < 0.05$, significantly different from the control group at the same time point.

Cell proliferation assay

After *C. pneumoniae* infection, the cells were seeded at 5.0×10^4 cells/well in a 96-well plate. The proliferation of infected cells was examined at 0, 24, 48, and 72 h after infection, using the Cell Counting Kit-8 (WST-8, Dojindo, Kumamoto, Japan) according to the manufacturer's instructions. Cell numbers and viabilities

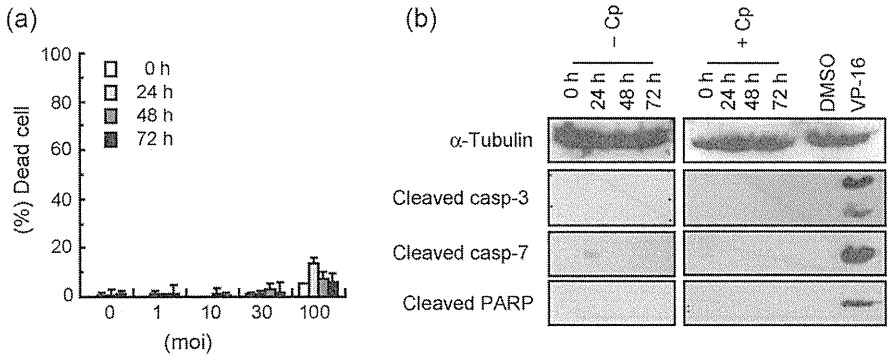

Fig. 2. Less activation of apoptosis machinery of the Jurkat cells infected by *C. pneumoniae*. (a) Jurkat cells were infected with *C. pneumoniae* at an m.o.i. of 0, 1, 10, 30, or 100. At 0, 24, 48, and 72 h after infection, cells were collected, and the dead cell ratios of the infected cells were measured. The ratios are represented as means ± standard deviations ($n = 3$). (b) Jurkat cells infected with *C. pneumoniae* at an m.o.i. of 0 or 30 were collected at 0, 24, 48 and 72 h after infection, protein extracts from the infected cells were subjected to immunoblotting with anti-α-tubulin, anti-cleaved caspase-3, anti-cleaved caspase-7 and anti-cleaved PARP antibodies. Representative results from 3 independent experiments are shown.

of the infected cells at these time-points were determined by the trypan-blue dye exclusion method.

Immunoblot analysis

Cell lysates were prepared in lysis buffer (50 mM Tris, HCl, pH 8.0, 150 mM NaCl, 10% glycerol, and 1% Triton X-100) containing protease inhibitor cocktail (Sigma) and phosphatase inhibitor cocktail (Sigma) (Hirai and Wang 2002). Equal protein amounts of the lysates were analyzed by SDS-PAGE and blotting using peroxidase conjugated secondary antibody and the SuperSignal West Dura Extended Duration Substrate (Thermo, Rockford, IL). Anti-α-tubulin monoclonal antibody was obtained from Sigma. Anti-cyclin D3 monoclonal antibody was purchased from BD. Anti-cleaved PARP polyclonal antibody, anti-cleaved caspase-3 polyclonal antibody, anti-cleaved caspase-7 polyclonal antibody, anti-p70S6K monoclonal antibody, anti-phospho-p70S6K monoclonal antibody, anti-AKT monoclonal antibody and anti-phospho-AKT monoclonal antibody were purchased from CST Japan (Tokyo, Japan).

Statistical analysis

Statistical analyses were performed using the unpaired Student's *t* test.

Results

The effect of C. pneumoniae infection on the proliferation of Jurkat cell proliferation

The number of Jurkat cells and their cell viability were examined at 0, 24, 48, and 72 h after infection (Fig. 1), to evaluate the effect of *C. pneumoniae* infection on the proliferation of Jurkat cells. The results showed that the proliferation of Jurkat cells was significantly suppressed by *C. pneumoniae* infection in an m.o.i.-dependent manner, and this suppression was most evident at the earlier time-points, within 24 h of infection. Similar results were obtained from the trypan blue dye exclusion assay (Fig. 1a) and the WST-8 cell proliferation assay (Fig. 1b).

In order to confirm whether the suppression of Jurkat cell proliferation by *C. pneumoniae* was cell type specific event, we performed similar WST-8 cell proliferation assay using human epithelial cell line HEp-2 cells (Fig. 1c). The results indicated that the infected HEp-2 cell proliferation was also suppressed by *C. pneumoniae* infection as same manner as the infected Jurkat cells. This result suggested that suppression of cell proliferation by *C. pneumoniae* was not cell type specific event.

The trypan blue dye exclusion assay showed that cell death caused by *C. pneumoniae* infection was minimal in Jurkat cells (Fig. 2a). To confirm this, cleaved caspase-3, cleaved caspase-7 and cleaved PARP were detected in the Jurkat cells infected with *C. pneumoniae* at an m.o.i. of 0 or 30 by immunoblotting (Fig. 2b). Any obvious signals corresponding to cleaved caspase-3, cleaved-caspase-7 and cleaved PARP were not observed from the Jurkat cells infected with *C. pneumoniae* at an m.o.i. of 30. Taken together, these results suggested that apoptosis was not induced in the Jurkat cells infected with *C. pneumoniae* at least up to an m.o.i. of 30.

The suppression of Jurkat cell proliferation is dependent on viable C. pneumoniae infection

To prove that *C. pneumoniae* infection was essential to the suppression of Jurkat cell proliferation, the cell proliferation assay using WST-8 after treatment of actin polymerization inhibitor, cytochalasin D were performed. Repeatedly, the proliferation of the Jurkat cells was suppressed by *C. pneumoniae* infection at an m.o.i. of 30. Cytochalasin D treatment itself did not effect on the Jurkat cell proliferation. Moreover, cytochalasin D restored the Jurkat cell proliferation even under presence of *C. pneumoniae* probably by blocking *C. pneumoniae* invasion into the host Jurkat cells (Fig. 3).

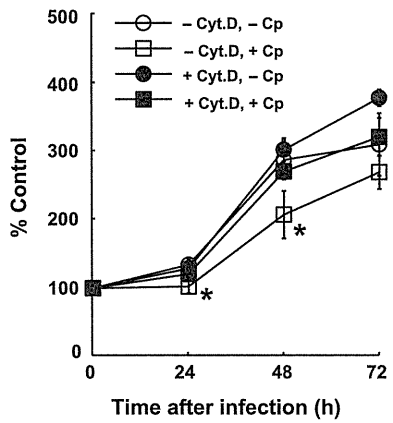

Fig. 3. *C. pneumoniae* infection-dependent suppression of the infected Jurkat cell proliferation. Jurkat cells were treated with or without 10 μM of cytochalasin D for 30 min and infected with or without *C. pneumoniae* at an m.o.i. of 30. At 0, 24, 48, and 72 h after infection, the relative viabilities of the infected Jurkat cells were measured. Representative results from 3 independent experiments are shown. The numbers indicate the value relative to the control group at time point 0, and are represented as means ± standard deviations ($n = 3$). *$P < 0.05$, significantly different from the control group at the same time point.

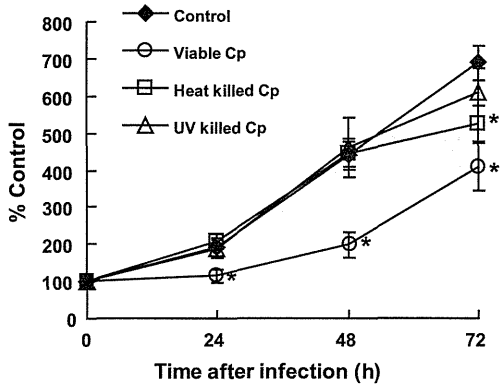

Fig. 4. Viable *C. pneumoniae*-dependent suppression of the infected Jurkat cell proliferation. Infection was performed with viable, heat-killed, or UV-killed *C. pneumoniae* at an m.o.i. of 10. At 0, 24, 48, and 72 h after exposure to the bacteria, aliquots of the Jurkat cells were harvested and subjected to the trypan-blue dye exclusion assay. Representative results from 3 independent experiments are shown. The values indicate the numbers relative to the control group at time point 0, and represent means ± standard deviations ($n = 3$). $^*P < 0.05$, significantly different from the control group at the same time point.

This result suggested that the suppression of Jurkat cell proliferation required the establishment of *C. pneumoniae* infection.

To evaluate whether the suppressive effect of *C. pneumoniae* on proliferation required viable *C. pneumoniae*, heat-killed and UV-killed *C. pneumoniae* were substituted for live bacteria in the proliferation assay (Fig. 4). Viable *C. pneumoniae* infection at an m.o.i. of 10 consistently suppressed the proliferation of infected Jurkat cells. In contrast, neither heat-killed nor UV-killed *C. pneumoniae* showed any suppressive effects on the proliferation of the host Jurkat cells. These data suggest that viable *C. pneumoniae* infection is essential to the suppression of proliferation observed in infected Jurkat cells.

The suppression of Jurkat cell proliferation by C. pneumoniae infection is accompanied by a reduction in phosphorylation level at Thr389 of p70S6K

Cyclin D3 is reported as key regulator in Jurkat cell proliferation (Boonen et al. 1999). Therefore, cyclin D3 protein level was evaluated by immunoblot analysis in order to determine whether suppression of Jurkat cell proliferation by *C. pneumoniae* infection involved cyclin D3 down modulation. As shown in Fig. 5a, cyclin D3 protein levels were diminished by *C. pneumoniae* infection. The reduction in cyclin D3 was an m.o.i. dependent (Fig. 5b) and required infection with viable *C. pneumoniae* (Fig. 5c). In spite of decreased cyclin D3 protein level, we could not observe an accumulation of infected Jurkat cells at Go/G1 phase (data not shown). This suggested that the suppression of Jurkat cell proliferation associated with *C. pneumoniae* infection did not involve the induction of cell cycle arrest at the G1 phase.

We performed preliminary experiments with chemical compounds including MEK inhibitor U0126, protein kinase A (PKA) activator CPT-cAMP, PKA inhibitor H-89, mammalian target of rapamycin (mTOR) inhibitor rapamycin. U0126, CPT-cAMP and rapamycin suppressed Jurkat cell proliferations; however, we could not obtain any evidence that MEK and PKA pathways were related to the suppression of cyclin D3 expression level. Therefore, we further analyzed phosphoinositide 3-kinase (PI3K)/AKT/mTOR/p70S6K pathway. This pathway is prominent signal transduction pathway in cell proliferation and growth (Asnaghi et al. 2004; Manning 2004; Peter et al. 2010), and *Chlamydia* infection stimulates phosphorylation of AKT by PI3K dependent manner (Coombes and Mahony 2002; Verbeke et al. 2006). Therefore, alteration of the phosphorylation status of AKT and p70S6K was investigated in the context of *C. pneumoniae* infection (Fig. 6). Even in the absence of *C. pneumoniae* infection, AKT was somewhat phosphorylated by stimulation with additional FCS after the procedure of *C. pneumoniae* infection. Consistent with previous report, phosphorylation on Thr308 and Ser473 of AKT was induced by *C. pneumoniae* infection. In case of p70S6K, Thr389 phosphorylation was induced by additional FCS as same manner as AKT; however, *C. pneumoniae* infection dramatically suppressed Thr389 phosphorylation of p70S6K in contrast to activation of AKT. Concurrently, cyclin D3 expression level was also suppressed as phosphorylation at Thr389 of p70S6K (Fig. 6). These data suggested that down modulation of the p70S6K phosphorylation by unidentified mechanism associated with *C. pneumoniae* infection could be the main mechanism for suppression of Jurkat cell proliferation.

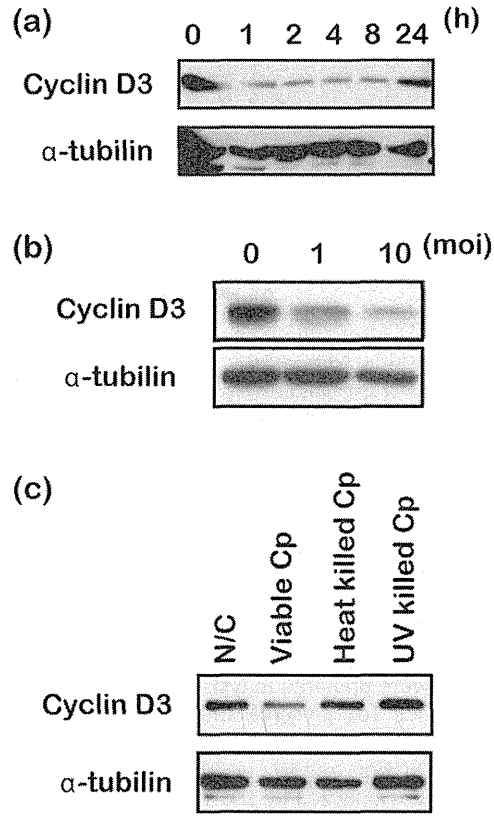

Fig. 5. Viable *C. pneumoniae* infection decreases cyclin D3 expression levels. (a) At 0, 1, 2, 4, 8, and 24 h after *C. pneumoniae* infection at an m.o.i. of 10, aliquots of infected Jurkat cells were harvested and lysed in an appropriate volume of lysis buffer. Equal protein amounts of the cell lysates were analyzed via immunoblotting, using anti-cyclin D3 antibody and anti-α-tubulin antibody. (b) Infected Jurkat cells were collected 2 h after *C. pneumoniae* infection at an m.o.i. of 0, 1, or 10. Equal protein amounts of the cell lysates were analyzed via immunoblotting using anti-cyclin D3 antibody and anti-α-tubulin antibody. (c) Jurkat cells were harvested 2 h after infection with viable *C. pneumoniae* at an m.o.i. of 10, or exposure to the same amount of heat-killed or UV-killed *C. pneumoniae*. Equal protein amounts of the cell lysates were subjected to immunoblotting analysis using anti-cyclin D3 and anti-α-tubulin antibodies.

Discussion

Previously, we have reported that *C. pneumoniae* derived antigens and DNA can be detected in PBMCs (Haranaga et al. 2001a,b), and that *C. pneumoniae* infects and multiplies in T lymphocytes (Haranaga et al. 2001a,b; Yamaguchi et al. 2002a,b, 2008). It has also been reported that *C. pneumoniae* infection affects host-cell function by reducing CD3 and CD25 expression levels (Yamaguchi et al. 2008; Hirai et al. 2010). However, how *C. pneumoniae* infection

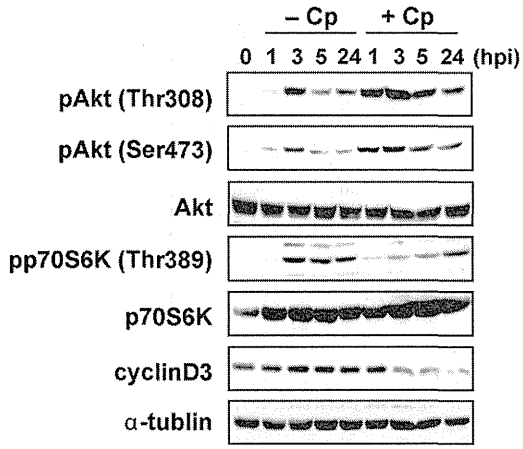

Fig. 6. Suppression of Thr398 phosphorylation of p70S6K by *C. pneumoniae* infection. Jurkat cells were harvested at the indicated time-points after infection with *C. pneumoniae* at an m.o.i. of 0 or 10. After preparation of cell lysates, equal protein amounts from each were subjected to immunoblotting analysis using anti-AKT, anti-phospho-AKT (Thr308), anti-phospho-AKT (Ser473), anti-p70S6K, anti-phospho-p70S6K (Thr389), anti-cyclin D3, and anti-α-tubulin antibodies.

modulates host-cell functions, and the effect these modulations have on the onset and progression of disease, is not well understood. In this study, we investigated the mechanism by which *C. pneumoniae* infection suppresses T lymphocyte proliferation using the human acute T cell lymphoma cell line, Jurkat E6-1 as a model.

Data obtained in this study indicate that Jurkat cell proliferation is suppressed by *C. pneumoniae* infection, which is consistent with our previous report (Hirai et al. 2010). A recent report suggests that *C. pneumoniae* inhibits proliferation of activated human T lymphocytes by inducing apoptosis (Olivares-Zavaleta et al. 2011). In this study, the lower live-to-dead cell ratios and the less activation of apoptosis machinery, such as cleaved caspase-3, were observed in the infected Jurkat cell cultures. Considering the same results obtained in the infected PBMCs in our previous study (Hirai et al. 2010), we hypothesized that the suppression of proliferation induced by *C. pneumoniae* infection might not be solely due to cell death (infection-induced apoptosis).

It has been reported that various agents can induce cell cycle arrest in T lymphocytes at the G0/G1 phase (Fei et al. 2009; Sharif et al. 2010; Koyanagi et al. 2007; Wilson et al. 2005; Dohda et al. 2007; Gutzkow et al. 2003). In addition, cyclin D3 is reportedly the critical G1 cyclin in a leukemic T cell line (Boonen et al. 1999; Casanovas et al. 2004). Reduction of cyclin D3 protein levels in Jurkat cells results in G1 arrest of the cells (Boonen et al. 1999; van Oirschot et al. 2001). Therefore, we investigated expression levels of cyclin D3 in Jurkat cells infected with *C. pneumoniae*. In the infected Jurkat cells, cyclin D3 protein level was down regulated in an m.o.i.-dependent manner, and it was reliant on exposure to viable *C. pneumoniae* bacteria (Fig. 4). However, contrary to our expectations, we did not observe marked G1 arrest in *C. pneumoniae* infected Jurkat cells (data not shown). These observations suggested that cyclin D3 was not the main target utilized by *C. pneumoniae* to suppress host cells proliferation, and that alternative suppression mechanisms were yet to be unveiled.

Despite the protein half-life of cyclin D3 protein being relatively short (De Santa et al. 2007), protein levels of cyclin D3, unlike cyclins B1, A, and E, are relatively stable throughout the entire cell cycle (Gong et al. 1995). This suggests that the down regulation of cyclin D3 protein levels observed in this study was probably due to transcriptional and/or translational retardation. By our preliminary investigation using semi-quantitative RT-PCR, it was indicated that mRNA levels of cyclin D3 were not being altered by *C. pneumoniae* infection. Furthermore, proteasome inhibitor, MG-132 treatment maintained protein level of cyclin D3 in the Jurkat cells infected with *C. pneumoniae* (data not shown). Therefore, we focused our investigations on probing essential signal transduction pathways for the translational regulation of cyclin D3 as an index of translation level in the Jurkat cells infected with *C. pneumoniae*.

Various reports have suggested that the signal transduction pathways responsible for Jurkat cell proliferation and cyclin D expression include the mitogen-activated protein (MAP) kinase pathway (Terada et al. 1999), the PKA pathway (Gutzkow et al. 2003; van Oirschot et al. 2001), and the mTOR pathway (Hleb et al. 2004). Among these pathways, our preliminary consideration with certain chemical compounds suggested mTOR pathway might be responsible for the suppression of Jurkat cell proliferation and cyclin D3 protein level by *C. pneumoniae* infection.

Various molecules are involved in protein translation, including the cascade consisting of PI3K, AKT, mTOR, p70S6K and translational control machineries (Ma and Blenis 2009; Tee and Blenis 2005). Downstream serine/threonine kinase, p70S6K, is a direct substrate of multi-component mTOR complex 1 (mTORC1), and activation of p70S6K is initiated by phosphorylation at Thr389 which is most correlated phosphorylation site with p70S6K activation (Weng et al. 1998). Activated p70S6K modulates translation-initiation-factor functions, to facilitate protein synthesis (Ma and Blenis 2009). Once activity of p70S6K is weakened by de-phosphorylation at Thr389, protein synthesis is also attenuated (Ma and Blenis 2009). Consistent with this, data obtained in this study showed that the lower phosphorylation status of p70S6K induced by *C. pneumoniae* infection was accompanied by lower expression levels of cyclin D3 (Fig. 6). However, phosphorylations at Thr308 and Ser473 of upstream AKT were still induced by *C. pneumoniae* infection as the previous report (Coombes and Mahony 2002). This discrepancy between phosphorylation status, i.e. activation status of AKT and p70S6K suggested suppression of Jurkat cell by *C. pneumoniae* might be mediated by regulatory mechanism surrounding mTORC1.

At present, many factors involved in the modulation of mTORC1 activity by *C. pneumoniae* remain to be explained. AMPK which is one of upstream kinases of mTOR is an important molecule for sensing intracellular energy and nutrition (Hardie 2011; Canto and Auwerx 2010). AMPK is activated when the concentration of intracellular ATP is lowered, and activated AMPK phosphorylates Raptor to inhibit association between Raptor and mTOR (Gwinn et al. 2008). Consequently, inactivation of mTORC1, dephosphorylation of p70S6K, retardation of protein synthesis, and cell cycle arrest occurs. Consistently, inhibition of AMPK by a chemical inhibitor restored phosphorylation level at Thr389 of p70S6K and cyclin D3 expression level even under *C. pneumonia* infection in our preliminary experiment. During the Chlamydial life cycle, host-cell ATP is consumed by the intracellular pathogen, and therefore, activation of AMPK associated with *C. pneumoniae* infection is highly plausible. Growth arrest and DNA damage protein 34 (Gadd34) was also reported as an inhibitor of mTOR molecule under host cellular energetic stress such as energy depletion, and virus infection (Watanabe et al. 2007; Minami et al. 2007). Additionally, it is well known that *C. pneumoniae* secretes effector proteins through the type 3 secretion system (Bailey et al. 2007; Subtil et al. 2001). In this regard, forced expression of Chlamydial effector protein, CopN, arrests the cell cycle at the G2/M phase (Huang et al. 2008). Therefore, the contribution of these Chlamydial secretion proteins should also be considered.

In conclusion, *C. pneumoniae* infection weakened p70S6K phosphorylation at Thr389 in the infected Jurkat cells. Consequently, the infected Jurkat cell proliferation was suppressed via attenuation of protein synthesis in earlier period after the infection. Further

details of the mechanisms of suppression induced by *C. pneumoniae* infection remain to be elucidated.

Acknowledgements

We wish to thank Ms. Haruka Yamaski and Ms. Mikako Ohashi for their excellent technical help. This work was supported by KAKENHI (23590505).

References

Airenne, S., Surcel, H.M., Alakarppa, H., Laitinen, K., Paavonen, J., Saikku, P., Laurila, A., 1999. *Chlamydia pneumoniae* infection in human monocytes. Infect. Immun. 67, 1445.

Asnaghi, L., Bruno, P., Priulla, M., Nicolin, A., 2004. mTOR: a protein kinase switching between life and death. Pharmacol. Res. 50, 545.

Bailey, L., Gylfe, A., Sundin, C., Muschiol, S., Elofsson, M., Nordstrom, P., Henriques-Normark, B., Lugert, R., Waldenstrom, A., Wolf-Watz, H., Bergstrom, S., 2007. Small molecule inhibitors of type III secretion in Yersinia block the *Chlamydia pneumoniae* infection cycle. FEBS Lett. 581, 587.

Boonen, G.J., van Oirschot, B.A., van Diepen, A., Mackus, W.J., Verdonck, L.F., Rijksen, G., Medema, R.H., 1999. Cyclin D3 regulates proliferation and apoptosis of leukemic T cell lines. J. Biol. Chem. 274, 34676.

Canto, C., Auwerx, J., 2010. AMP-activated protein kinase and its downstream transcriptional pathways. Cell. Mol. Life Sci. 67, 3407.

Casanovas, O., Jaumot, M., Paules, A.B., Agell, N., Bachs, O., 2004. P38SAPK2 phosphorylates cyclin D3 at Thr-283 and targets it for proteasomal degradation. Oncogene 23, 7537.

Coombes, B.K., Mahony, J.B., 2002. Identification of MEK- and phosphoinositide 3-kinase-dependent signalling as essential events during *Chlamydia pneumoniae* invasion of HEp2 cells. Cell. Microbiol. 4, 447.

De Santa, F., Albini, S., Mezzaroma, E., Baron, L., Felsani, A., Caruso, M., 2007. pRb-dependent cyclin D3 protein stabilization is required for myogenic differentiation. Mol. Cell. Biol. 27, 7248.

Dohda, T., Maljukova, A., Liu, L., Heyman, M., Grander, D., Brodin, D., Sangfelt, O., Lendahl, U., 2007. Notch signaling induces SKP2 expression and promotes reduction of p27Kip1 in T-cell acute lymphoblastic leukemia cell lines. Exp. Cell Res. 313, 3141.

Fei, F., Yu, Y., Schmitt, A., Rojewski, M.T., Chen, B., Gotz, M., Dohner, H., Bunjes, D., Schmitt, M., 2009. Dasatinib inhibits the proliferation and function of CD4+CD25+regulatory T cells. Br. J. Haematol. 144, 195.

Gaydos, C.A., Summersgill, J.T., Sahney, N.N., Ramirez, J.A., Quinn, T.C., 1996. Replication of *Chlamydia pneumoniae* in vitro in human macrophages, endothelial cells, and aortic artery smooth muscle cells. Infect. Immun. 64, 1614.

Geng, Y., Shane, R.B., Berencsi, K., Gonczol, E., Zaki, M.H., Margolis, D.J., Trinchieri, G., Rook, A.H., 2000. *Chlamydia pneumoniae* inhibits apoptosis in human peripheral blood mononuclear cells through induction of IL-10. J. Immunol. 164, 5522.

Godzik, K.L., O'Brien, E.R., Wang, S.K., Kuo, C.C., 1995. In vitro susceptibility of human vascular wall cells to infection with *Chlamydia pneumoniae*. J. Clin. Microbiol. 33, 2411.

Gong, J., Traganos, F., Darzynkiewicz, Z., 1995. Growth imbalance and altered expression of cyclins B1, A, E, and D3 in MOLT-4 cells synchronized in the cell cycle by inhibitors of DNA replication. Cell Growth Differ. 6, 1485.

Grayston, J.T., 2000. Background and current knowledge of *Chlamydia pneumoniae* and atherosclerosis. J. Infect. Dis. 181 (Suppl. 3), S402.

Gutzkow, K.B., Lahne, H.U., Naderi, S., Torgersen, K.M., Skalhegg, B., Koketsu, M., Uehara, Y., Blomhoff, H.K., 2003. Cyclic AMP inhibits translation of cyclin D3 in T lymphocytes at the level of elongation by inducing eEF2-phosphorylation. Cell. Signal. 15, 871.

Gwinn, D.M., Shackelford, D.B., Egan, D.F., Mihaylova, M.M., Mery, A., Vasquez, D.S., Turk, B.E., Shaw, R.J., 2008. AMPK phosphorylation of raptor mediates a metabolic checkpoint. Mol. Cell 30, 214.

Haranaga, S., Yamaguchi, H., Friedman, H., Izumi, S., Yamamoto, Y., 2001a. *Chlamydia pneumoniae* infects and multiplies in lymphocytes in vitro. Infect. Immun. 69, 7753.

Haranaga, S., Yamaguchi, H., Leparc, G.F., Friedman, H., Yamamoto, Y., 2001b. Detection of *Chlamydia pneumoniae* antigenin PBMNCs of healthy blood donors. Transfusion (Paris) 41, 1114.

Hardie, D.G., 2011. Sensing of energy and nutrients by AMP-activated protein kinase. Am. J. Clin. Nutr. 93, 891S.

Hirai, I., Wang, H.G., 2002. A role of the C-terminal region of human Rad9 (hRad9) in nuclear transport of the hRad9 checkpoint complex. J. Biol. Chem. 277, 25722.

Hirai, I., Utsumi, M., Yamaguchi, H., Yamamoto, Y., 2010. *Chlamydia pneumoniae* infection suppresses *Staphylococcus enterotoxin* B-induced proliferation associated with down-expression of CD25 in lymphocytes. Can. J. Microbiol. 56, 289.

Hleb, M., Murphy, S., Wagner, E.F., Hanna, N.N., Sharma, N., Park, J., Li, X.C., Strom, T.B., Padbury, J.F., Tseng, Y.T., Sharma, S., 2004. Evidence for cyclin D3 as a novel target of rapamycin in human T lymphocytes. J. Biol. Chem. 279, 31948.

Huang, J., Lesser, C.F., Lory, S., 2008. The essential role of the CopN protein in *Chlamydia pneumoniae* intracellular growth. Nature 456, 112.

Kalayoglu, M.V., Perkins, B.N., Byrne, G.I., 2001. *Chlamydia pneumoniae*-infected monocytes exhibit increased adherence to human aortic endothelial cells. Microbes Infect. 3, 963.

Koyanagi, M., Fukada, K., Uchiyama, T., Yagi, J., Arimura, Y., 2007. Long-term exposure to superantigen induces p27Kip1 and Bcl-2 expression in effector memory CD4+T cells. Cell. Immunol. 248, 77.

Ma, X.M., Blenis, J., 2009. Molecular mechanisms of mTOR-mediated translational control. Nat. Rev. Mol. Cell Biol. 10, 307.

Manning, B.D., 2004. Balancing Akt with S6K: implications for both metabolic diseases and tumorigenesis. J. Cell Biol. 167, 399.

Minami, K., Tambe, Y., Watanabe, R., Isono, T., Haneda, M., Isobe, K., Kobayashi, T., Hino, O., Okabe, H., Chano, T., Inoue, H., 2007. Suppression of viral replication by stress-inducible GADD34 protein via the mammalian serine/threonine protein kinase mTOR pathway. J. Virol. 81, 11106.

Mussa, F.F., Chai, H., Wang, X., Yao, Q., Lumsden, A.B., Chen, C., 2006. *Chlamydia pneumoniae* and vascular disease: an update. J. Vasc. Surg. 43, 1301.

Olivares-Zavaleta, N., Carmody, A., Messer, R., Whitmire, W.M., Caldwell, H.D., 2011. *Chlamydia pneumoniae* inhibits activated human T lymphocyte proliferation by the induction of apoptotic and pyroptotic pathways. J. Immunol. 186, 7120.

Peter, C., Waldmann, H., Cobbold, S.P., 2010. mTOR signalling and metabolic regulation of T cell differentiation. Curr. Opin. Immunol. 22, 655.

Quinn, T.C., Gaydos, C.A., 1999. In vitro infection and pathogenesis of *Chlamydia pneumoniae* in endovascular cells. Am. Heart J. 138, S507.

Sharif, T., Auger, C., Alhosin, M., Ebel, C., Achour, M., Etienne-Selloum, N., Fuhrmann, G., Bronner, C., Schini-Kerth, V.B., 2010. Red wine polyphenols cause growth inhibition and apoptosis in acute lymphoblastic leukaemia cells by inducing a redox-sensitive up-regulation of p73 and down-regulation of UHRF1. Eur. J. Cancer 46, 983.

Subtil, A., Parsot, C., Dautry-Varsat, A., 2001. Secretion of predicted Inc proteins of *Chlamydia pneumoniae* by a heterologous type III machinery. Mol. Microbiol. 39, 792.

Takano, R., Yamaguchi, H., Sugimoto, S., Nakamura, S., Friedman, H., Yamamoto, Y., 2005. Cytokine response of lymphocytes persistently infected with *Chlamydia pneumoniae*. Curr. Microbiol. 50, 160.

Tee, A.R., Blenis, J., 2005. mTOR, translational control and human disease. Semin. Cell Dev. Biol. 16, 29.

Terada, Y., Inoshita, S., Nakashima, O., Kuwahara, M., Sasaki, S., Marumo, F., 1999. Regulation of cyclin D1 expression and cell cycle progression by mitogen-activated protein kinase cascade. Kidney Int. 56, 1258.

van Oirschot, B.A., Stahl, M., Lens, S.M., Medema, R.H., 2001. Protein kinase A regulates expression of p27(kip1) and cyclin D3 to suppress proliferation of leukemic T cell lines. J. Biol. Chem. 276, 33854.

Verbeke, P., Welter-Stahl, L., Ying, S., Hansen, J., Hacker, G., Darville, T., Ojcius, D.M., 2006. Recruitment of BAD by the *Chlamydia trachomatis* vacuole correlates with host-cell survival. PLoS Pathog. 2, e45.

Watanabe, R., Tambe, Y., Inoue, H., Isono, T., Haneda, M., Isobe, K., Kobayashi, T., Hino, O., Okabe, H., Chano, T., 2007. GADD34 inhibits mammalian target of rapamycin signaling via tuberous sclerosis complex and controls cell survival under bioenergetic stress. Int. J. Mol. Med. 19, 475.

Watson, C., Alp, N.J., 2008. Role of *Chlamydia pneumoniae* in atherosclerosis. Clin. Sci. (Lond.) 114, 509.

Weng, Q.P., Kozlowski, M., Belham, C., Zhang, A., Comb, M.J., Avruch, J., 1998. Regulation of the p70 S6 kinase by phosphorylation in vivo. Analysis using site-specific anti-phosphopeptide antibodies. J. Biol. Chem. 273, 16621.

Wilson, K.C., Cattel, D.J., Wan, Z., Rahangdale, S., Ren, F., Kornfeld, H., Sullivan, B.A., Cruikshank, W.W., Center, D.M., 2005. Regulation of nuclear Prointerleukin-16 and p27(Kip1) in primary human T lymphocytes. Cell. Immunol. 237, 17.

Yamaguchi, H., Haranaga, S., Friedman, H., Moor, J.A., Muffly, K.E., Yamamoto, Y., 2002a. A *Chlamydia pneumoniae* infection model using established human lymphocyte cell lines. FEMS Microbiol. Lett. 216, 229.

Yamaguchi, H., Haranaga, S., Widen, R., Friedman, H., Yamamoto, Y., 2002b. *Chlamydia pneumoniae* infection induces differentiation of monocytes into macrophages. Infect. Immun. 70, 2392.

Yamaguchi, H., Yamada, M., Uruma, T., Kanamori, M., Goto, H., Yamamoto, Y., Kamiya, S., 2004. Prevalence of viable *Chlamydia pneumoniae* in peripheral blood mononuclear cells of healthy blood donors. Transfusion (Paris) 44, 1072.

Yamaguchi, H., Matsuo, J., Sugimoto, S., Utsumi, M., Yamamoto, Y., 2008. Inhibition of lymphocyte CD3 expression by *Chlamydophila pneumoniae* infection. Microb. Pathog. 45 (4), 290–296.

J Mol Model (2013) 19:465–475
DOI 10.1007/s00894-012-1560-7

ORIGINAL PAPER

Discovery of novel low-molecular-weight HIV-1 inhibitors interacting with cyclophilin A using in silico screening and biological evaluations

Yu-Shi Tian · Chris Verathamjamras · Norihito Kawashita · Kousuke Okamoto · Teruo Yasunaga · Kazuyoshi Ikuta · Masanori Kameoka · Tatsuya Takagi

Received: 4 June 2012 / Accepted: 2 August 2012 / Published online: 5 September 2012

Abstract Cyclophilin A has attracted attention recently as a new target of anti-human immunodeficiency virus type 1 (HIV-1) drugs. However, so far no drug against HIV-1 infection exhibiting this mechanism of action has been approved. To identify new potent candidates for inhibitors, we performed in silico screening of a commercial database of more than 1,300 drug-like compounds by using receptor-based docking studies. The candidates selected from docking studies were subsequently tested using biological assays to assess anti-HIV activities. As a result, two compounds were identified as the most active. Specifically, both exhibited anti-HIV activity against viral replication at a low concentration and relatively low cytotoxicity at the effective concentration inhibiting viral growth by 50 %. Further modification of these molecules may lead to the elucidation of potent inhibitors of HIV-1.

Keywords Drug design · In silico screening · Anti-HIV · Cyclophilin A · Inhibitor

Yu-Shi Tian and Chris Verathamjamras contributed equally to this work.

Y.-S. Tian · N. Kawashita · K. Okamoto · T. Takagi (✉)
Graduate School of Pharmaceutical Sciences, Osaka University,
1-6 Yamadaoka,
Suita, Osaka 565-0871, Japan
e-mail: ttakagi@phs.osaka-u.ac.jp

C. Verathamjamras · M. Kameoka (✉)
Thailand-Japan Research Collaboration Center on Emerging and Re-emerging Infections (RCC-ERI),
Building 10, Department of Medical Sciences,
Ministry of Public Health, Tiwanon Rd.,
Muang, Nonthaburi 11000, Thailand
e-mail: mkameoka@biken.osaka-u.ac.jp

N. Kawashita · T. Yasunaga · T. Takagi
Genome Information Research Center, Research Institute for Microbial Diseases, Osaka University,
3-1 Yamadaoka,
Suita, Osaka 565-0871, Japan

K. Ikuta · M. Kameoka
Department of Virology, Research Center for Infectious Disease Control, Research Institute for Microbial Diseases,
Osaka University,
3-1 Yamadaoka,
Suita, Osaka 565-0871, Japan

Introduction

Cyclophilin A (CypA) was discovered originally as the receptor of the immunosuppressive drug cyclosporin A (CsA)—a molecule exhibiting multiple biological functions. The formation of complexes between CypA and CsA, which is an 11-mer cyclic peptide isolated from the fungus *Tolypocladium inflatum*, allows CypA to interact with calcineurin, reduce the production of interferon γ and interleukin-2, and exert immunosuppressive effects [1]. CypA is one of 15 known human cyclophilins, and can catalyze cis–trans isomerization in peptide bonds containing proline via its peptidyl prolyl isomerase (PPIase) activity. Recently, it was reported that CypA interacts with the NS5A and NS5B parts of hepatitis C virus polymerase [2, 3], the nucleocapsid protein of the SARS coronavirus [4], and the capsid (CA) protein of human immunodeficiency virus type 1 (HIV-1) [5]. These multiple functions make CypA an attractive target for drug development.

In addition to CsA, the natural product sanglifehrin A [6] and several peptide analogs [7] were reported to be active inhibitors of CypA. Recently, to decrease HIV-1 infectivity by disrupting the interaction of CypA with CA, several small molecules have been developed [8, 9]. However,

new drugs against HIV-1 infection exhibiting this mechanism of action have not yet been approved.

Nevertheless, there are several published reports of structural information regarding to the binding modes of CypA and CA fragments [10], CsA [11], or small peptides [12], and the available information suggests the potential applicability of in silico inhibitor screening and design for elucidating potential inhibitors. Here, we screened a small database of 1,377 small-molecular-weight compounds. A total of 29 compounds was selected according to docking scores. Together with two commercial positive control compounds, these 29 selected compounds were tested using biological assays. Finally, two compounds were identified as potent anti-HIV candidates, displaying acceptable cellular toxicity.

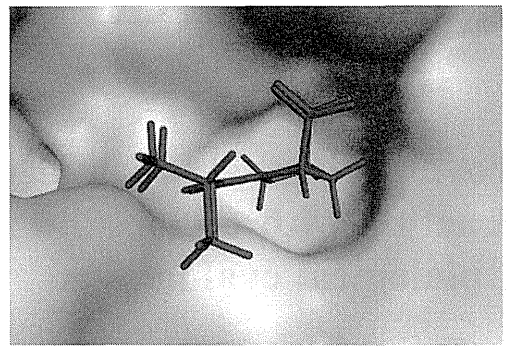

Fig. 2 Comparison of the re-docked conformation of AP with the crystallographic conformation in the CypA/AP complex. *Blue* Re-docked conformation, *red* crystallographic conformation. The root mean squared deviation (RMSD) between the two conformations was as low as 0.261 Å. The surface of the receptor is colored according to lipophilicity. *Green* Hydrophobic areas, *pink* hydrophilic areas

Materials and methods

Small molecular database for virtual screening

The structures of 1,377 low-molecular-weight compounds in a chemical structure data (SD) file format were obtained from ChemGenesis (http://www.all-chemy.com/), who supplied all the compound samples in the file. This SD file was converted into Molecular Operating Environment (MOE; Chemical Computing Group, Montreal, Canada) database format, and energy optimization of each molecule was performed under the MMFF94x forcefield using the MOE software package. The descriptors of molecular weight, lip_violation, lip_druglike [13], and diameter were calculated and typed into the fields of the database to confirm the basic properties of the compounds in the database.

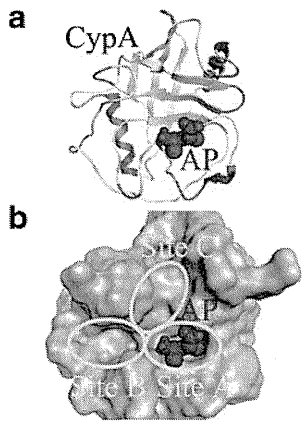

Fig. 1a,b The structure of receptor cyclophilin A (CypA) and its binding sites. **a** Representation of the dipeptide alanine-proline (AP, *red*) inside the CypA active site cavity. CypA adopts an eight-stranded antiparallel beta barrel structure, and AP is buried deeply in one of the cavities on the surface of CypA. The structure was obtained from 2CYH.pdb, and the figure was created by Molecular Operating Environment (MOE; Chemical Computing Group, Montreal, Canada) software. **b** Three docking sites on the surface of CypA. *Site A* is also known as the CypA MVA11-binding pocket, and AP also binds here. *Site B* is a hydrophobic pocket that is also known as the CypA Abu2-binding pocket. Above these two sites, there is some space, which we call *Site C* in this paper

Preparation of ligands and protein

The 1.64-Å resolution crystallographic data of CypA in complex with the dipeptide alanine-proline (AP; PDB entry 2CYH) [12] was obtained from the Brookhaven Protein Data Bank (http://www.pdb.org/pdb). This co-crystallized structure was used in preliminary studies to determine whether the docking parameters used were appropriate, and the structure of CypA within the structure was used as a receptor for screening the Allchemy database. In the present study, the "MOE dock" program was used to perform all the screening procedures. The Protonate3D module in MOE was used to assign ionization states, and to position hydrogen atoms into

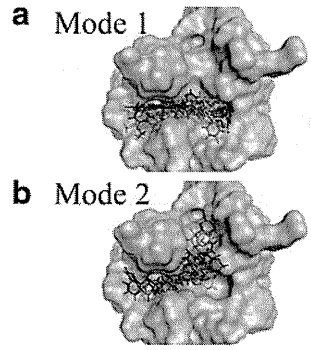

Fig. 3a,b Control compounds D4 and FD8 and 29 selected compounds docked into the surface sites of CypA. **a** Mode 1: lowest scored pose of each compound covered the region of Site A and Site B. **b** Mode 2: lowest scored pose of each compound docked into Site B and Site C, but not Site A

the receptor molecule. Subsequently, after adding partial charges under the MMFF94x forcefield and fixing the backbone atoms, energy minimization of the receptor was performed.

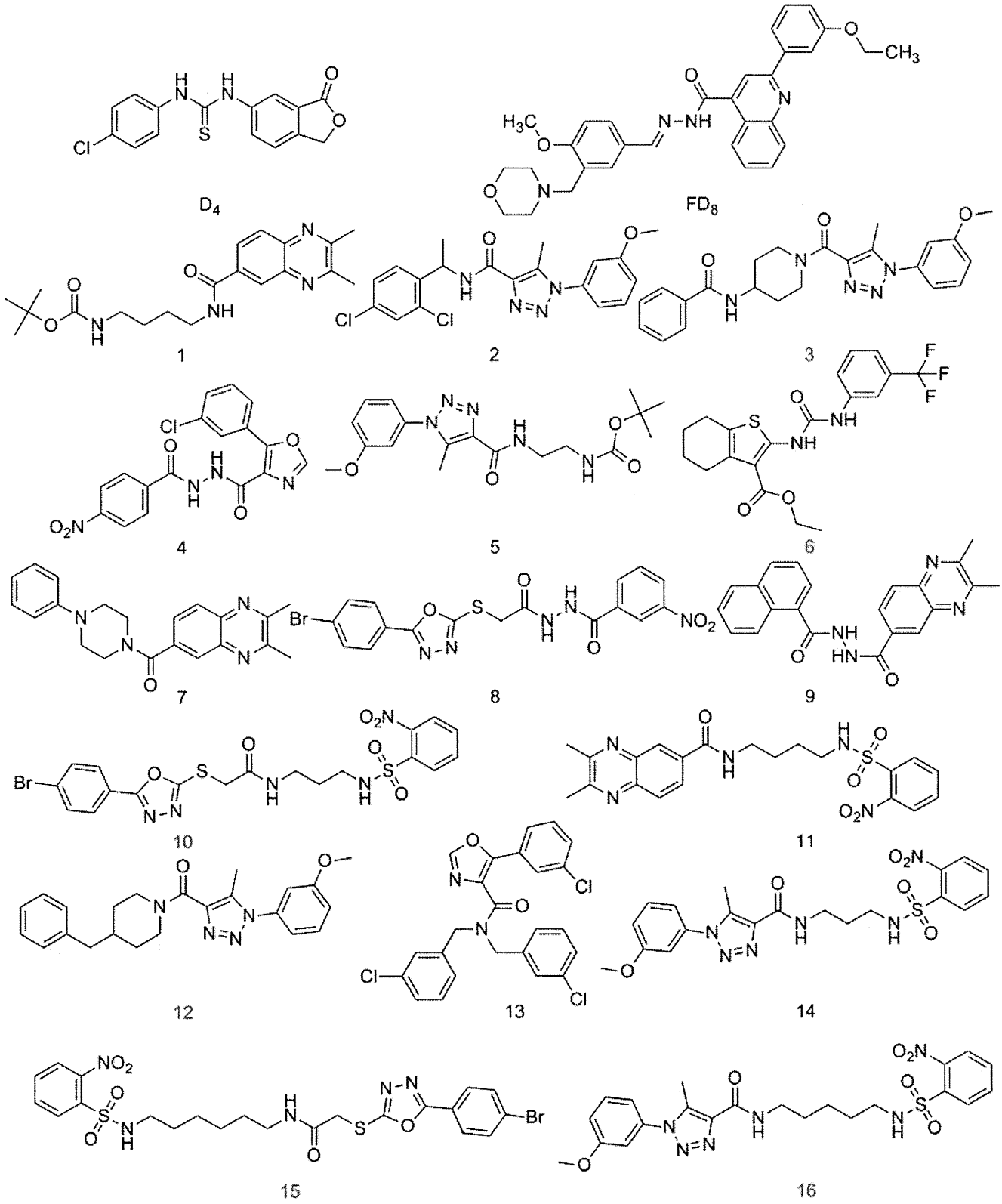

Fig. 4 Structures of compounds selected from the docking studies and the control compounds (D4 and FD8). The identifiers of compounds docking in Mode 1 poses are in *black*, and those of compounds docking in Mode 2 poses are in *blue*

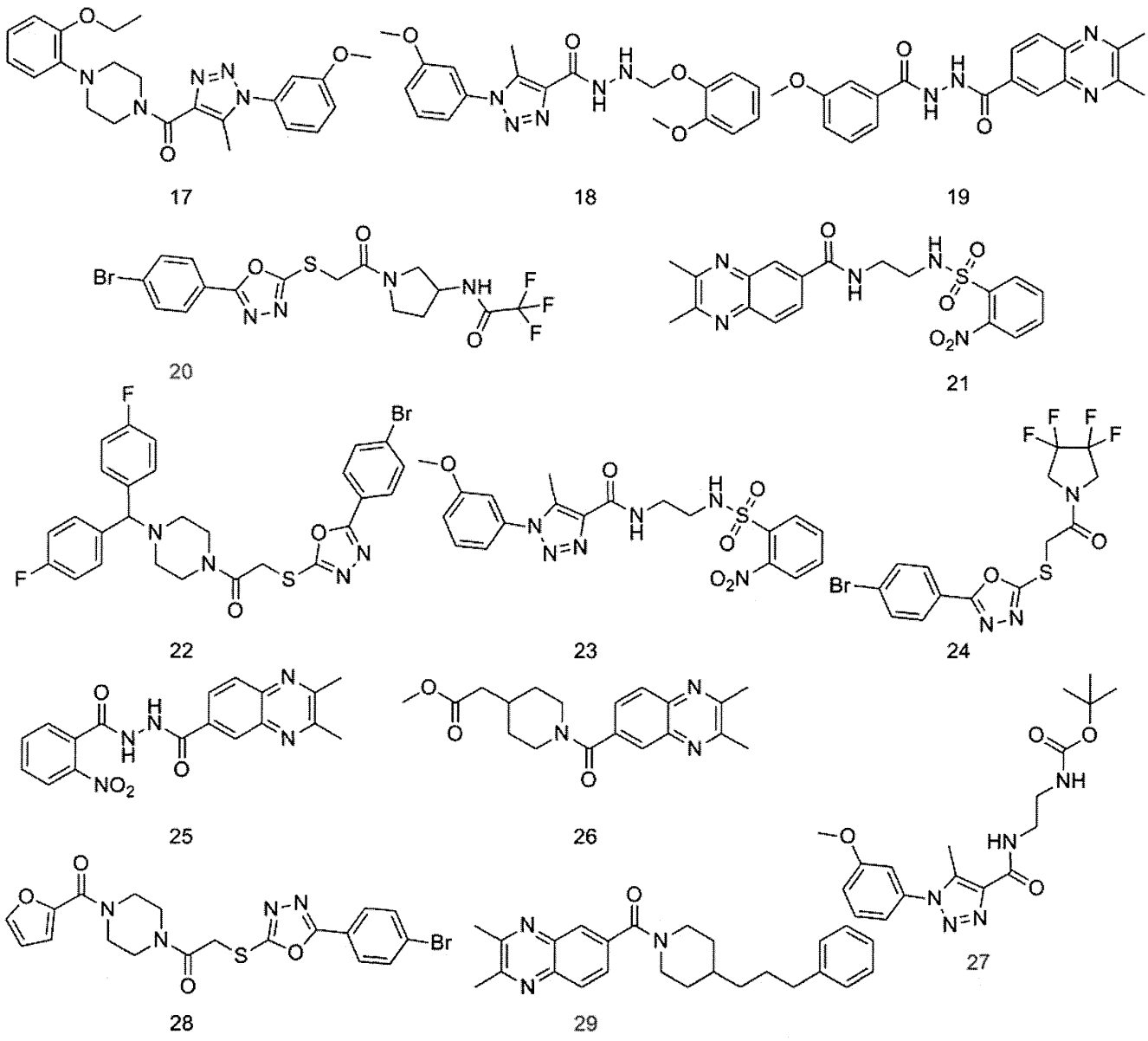

Fig. 4 (continued)

An active site covering the entire area of the two pockets in the CypA molecule was found using the SiteFinder module in MOE, and dummy atoms with hydrophobic or hydrophilic properties were placed into the two pockets to define the site.

Molecular docking

We docked AP back into the receptor (self-docking or re-docking) and screened the prepared database. For simplicity, flexibility of all of ligand atoms was allowed, in contrast to the receptor atoms during docking studies. We used five stages of the MOE Dock module to determine the potential docking poses of each ligand: (1) Dock was used to generate conformations from a single 3D conformer by applying a collection of preferred torsion angles to the rotatable bonds. Here, a systematic search was conducted covering all combinations of angles on a grid if this resulted in fewer than 5,000 conformers. Otherwise, a stochastic sampling of conformations was conducted. (2) The collection of poses was generated from the pool of ligand conformations using the Triangle Matcher method, which can align ligand triplets of atoms on triplets of alpha spheres in a relatively systematic way. (3) Poses generated by the placement methodology were rescored using the London dG scoring function, and low scores were assigned to good poses. The top 30 poses were kept. (4) These 30 poses were refined using the explicit molecular mechanics forcefield method; at this time, the forcefield was set to MMFF94x. (5) Poses resulting from the refinement stage were rescored using the London dG scoring function. The top 30 poses of each compound were

retained for manual examination. Finally, candidates used for examination were selected according to the best docking score of each compound.

Inhibition of HIV-1 replication

Compounds were obtained from ChemGenesis, and positive control compounds were purchased from Namiki Shoji (http://www.namiki-s.co.jp/). Biological assays were performed to determine whether the compounds exert inhibitory effects on a single replication cycle of HIV-1. Briefly, 293T cells (1.5×10^6 cells in a 100-mm dish) were transfected with 8.9 μg of the pNL4-3-based [14], envelope glycoprotein-deficient HIV-1 proviral construct carrying a luciferase reporter gene, pNL-Luc-E$^-$R$^+$ [15], together with 1.1 μg of a vesicular stomatitis virus G protein (VSVG) expression plasmid, pHit/G [16], using FuGENE HD transfection reagent (Roche, Basel, Switzerland) to generate VSVG-pseudotyped HIV-1. Eighteen

Table 1 The screening results of 29 test compounds and two positive controls

Compound	Concentration [μM]	Inhibitory effect on HIV-1 replication[a]	Cytotoxicity[b]	Solubility[c]	Docking score[d]
1	40	−	−	−	−10.75
2	11	−	+	−	−10.69
3	30	−	+	−	−10.62
4	9	++	−	+	−10.61
5	12.5	−	+	−	−10.58
6	10	+	+	−	−10.58
7	40	−	−	−	−10.48
8	40	−	−	+	−10.41
9	40	−	+	+	−10.39
10	10	−	+	+	−10.35
11	40	−	+	−	−10.31
12	10	++	+	−	−10.29
13	6	−	+	−	−10.27
14	9	−	+	−	−10.26
15	10	−	+	+	−10.23
16	5	−	+	−	−10.22
17	10	−	+	−	−10.21
18	12.5	−	+	−	−10.20
19	40	−	+	−	−10.14
20	40	−	+	+	−10.11
21	40	−	+	−	−10.10
22	20	−	−	+	−10.10
23	9	++	+	−	−10.09
24	40	−	−	+	−10.09
25	40	−	−	−	−10.05
26	40	−	−	−	−10.03
27	40	−	+	−	−10.01
28	10	−	+	+	−10.00
29	10	−	+	−	−10.00
D4[e]	40	++	−	−	NC[f]
FD8[e]	40	++	−	−	NC[f]

[a] Viral replication was more than 30 % inhibited judging by the reduction of luciferase activity, which was not obviously due to the cytotoxicity of the compound, in both U87.CD4.CXCR4 and MT4 cell lines (++), in either cell line (+) or in neither cell line (−)

[b] The viability of 293T, U87.CD4.CXCR4, and/or MT4 cells was more (−) or less than 70 % (+) in the presence of the compound at 40 μM

[c] Presence (+) or absence (−) of crystals in DMEM medium containing 0.2 % DMSO

[d] The score was calculated by MOE

[e] Control compounds

[f] Not calculated

hours later, the transfected 293T cells were trypsinized and split into 200-μl subcultures in a 96-well plate in the presence of the indicated concentrations of a test compound. After 30 h of incubation, the cell culture supernatant was used to infect subconfluent U87.CD4.CXCR4 [17] or MT-4 cells treated with the corresponding compound. Twenty-four hours after infection, the luciferase activity in infected cells was measured using the Steady Glo Luciferase assay kit (Promega, Madison, WI) with a microplate luminometer (LB960, Berthold, Bad Wildbad, Germany) according to the manufacturer's protocol. The inhibitory effect of the compounds on viral replication was evaluated as the reduction in luciferase activity in infected cells. In addition, a cell toxicity test was performed using the WST-1 cell proliferation assay system (Roche) according to the manufacturer's protocol. Briefly, subconfluent 293T, U87.CD4.CXCR4, and MT-4 cells were treated with the indicated concentrations of a compound for 24 h. WST-1 reagent was then added to the cell culture, which was further incubated until the absorbance of the samples at 450 nm was approximately 1.4 (approximately 1 h for 293T and U87.CD4.CXCR4 cells and 3 h for MT-4). The absorbance of the samples was measured using a microplate reader (Multiskan FC, Thermo Scientific, Rockford, IL), and the cytotoxicity of the compounds was evaluated as a reduction in absorbance. U87.CD4.CXCR4 cells were obtained through the AIDS Research and Reference Reagent Program (Division of AIDS, NIAID, NIH) from HongKui Deng and Dan R. Littman.

Structural analysis and residue interaction analysis

The interaction modes of the best poses of selected ligands were assessed using the Ligand Interactions module in MOE. The distances between important residues and ligands were measured. Subsequently, the best docking poses of active compounds in complex with

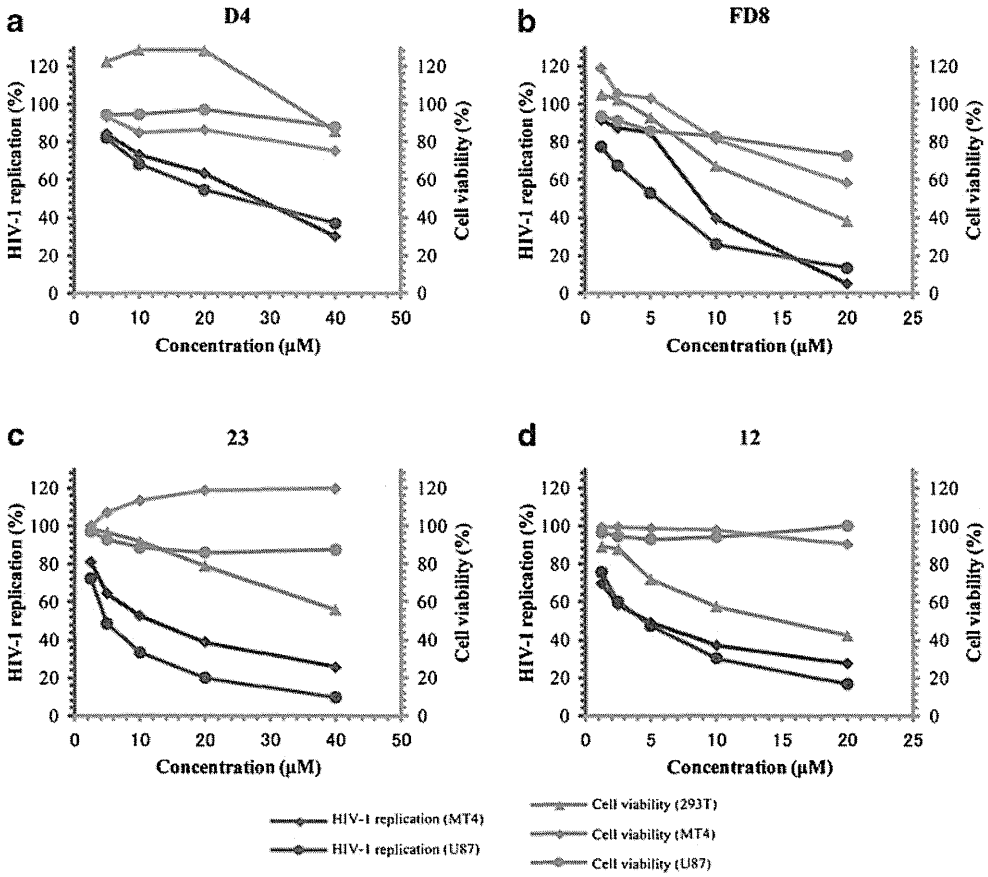

Fig. 5 Inhibitory effects on human immunodeficiency virus type 1 (HIV-1) replication and cellular toxicities of active compounds and controls. A vesicular stomatitis virus G protein-pseudotyped reporter virus was produced from 293T cells transfected with proviral DNA in the presence of various concentrations of the compound indicated. U87.CD4.CXCR4 or MT-4 cells were treated with a corresponding compound and then infected with the virus produced in the culture supernatant of 293T cells. Twenty-four hours after infection, the luciferase activity of infected cells was measured. The results are expressed as a percentage of viral replication, which was calculated by determining the reduction in luciferase activity in the presence of a compound compared with that in the control experiment in the absence of the compound. All data points represent the means of two to four independent experiments. In addition, the cytotoxicity of each compound was measured using WST-1 reagent. The cytotoxicity of each compound is expressed as a percentage of the reduction in the absorbance in the presence of the compound

CypA were analyzed using IF-E 6.0 [18] (created by Dr. Hooman Shadnia at Carleton University), retrievable from the SVL exchange service. As mentioned in reports by Shadnia and others [18, 19], IF-E 6.0 can partition the native forcefield potentials and derive net interaction forces. It is used to decompose the interaction forces into three dimensions while analyzing the per-residue interactions. A list of positive and negative interaction energy values between a ligand and its neighbor receptor residues (within a defined distance range) can be calculated; negative values indicate favorable interactions, whereas positive values indicate unfavorable interactions. For our candidate ligands, receptor residues oriented less than 4.5 Å were analyzed.

Results and discussion

In silico screening

Comparison between X-ray crystal structure and structure determined by docking

To ensure the validity of our docking procedures and docking parameters before screening, we performed a test using the co-crystallographic data (pdb identifier: 2CYH) of CypA and AP (Fig. 1) [12]. AP was isolated from the complex and then re-docked into the receptor CypA using the MOE software package. The best docking pose to emerge from our docking differed from the original conformation only by 0.261 Å in root mean square deviation (RSMD). Therefore, we selected the pose displaying the lowest docking score as the best pose. Figure 2 shows the comparison between the X-ray crystal structure (colored in red) of AP and the best docking pose (colored in blue).

Basic properties of compounds in the target database

We selected a commercially available database from ChemGenesis (http://www.all-chemy.com/) containing 1,377 low-molecular-weight compounds as the source database. The drug-likeness of these compounds was calculated by the QuaSAR-Descriptor module in MOE. More than 85 % of the compounds obeyed drug-likeness (the number of violations of Lipinski's Rule of Five [13] was less than two). Although less drug-like compounds are usually removed from the target database before docking, because of the small number of compounds in the database, both drug-like and less drug-like compounds were tested. The calculated molecular weights of compounds varied between 201.2 and 622.8 Da, and 1,325 compounds had molecular weights of less than 500 Da. According to the pocket size of CypA, the diameters of the compounds, which varied between 7 and 30 Å, were considered suitable, and no compounds were rejected before performing docking studies.

Analysis of receptor properties and definition of docking sites

According to the co-crystal data of CypA/AP, CypA adopts an eight-stranded antiparallel beta barrel structure (Fig. 1a), and AP is buried deeply in one of the cavities on the surface of CypA (Fig. 1b). This cavity is also where CsA, the HIV CA fragment, and other substrates bind. The most important residues of this cavity were identified by site-directed mutagenesis (Arg55, Phe60, Phe113, and His126) [20]. This cavity has also been called Site A or the MVA11-binding pocket (according to CsA binding mode) in previous reports [8, 21]. Over a saddle-like region, there is another hydrophobic pocket called Site B, or the Abu2-binding pocket. In addition to Sites A and B, there is also some empty space above, referred to here as Site C (Fig. 1b). Although the co-crystallographic data of the CypA/CA fragment indicate that Site A should be the direct docking site, Sites B or C could be considered an auxiliary cavity when compounds possess important elongated functional groups. Therefore, using the SiteFinder module in MOE, we defined a larger docking region contained among Sites A, B and C, and docked compounds in the target database into CypA.

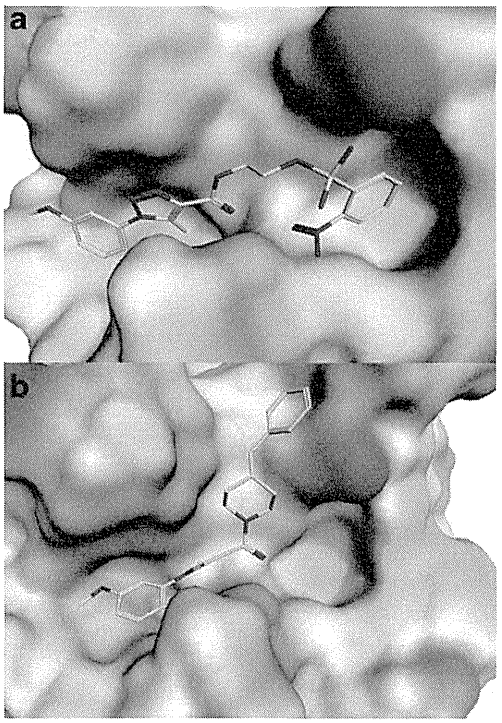

Fig. 6a,b Docking poses of two active compounds: **23** and **12**. **23** binds using Mode 1 (**a**), and **12** binds using Mode 2 (**b**)

Selection of compounds for biological evaluation

According to the predicted fitting score, which expresses the lowest binding energy of a certain pose, we selected 29 compounds, as shown in Figs. 3, and two previously reported active compounds as controls [8, 22]. We observed two binding modes: (1) molecules covering both Site A and Site B; and (2) molecules placed into Site B and Site C, but not Site A (Fig. 4). Of the 29 compounds listed in Fig. 3, 20 bound in the style of Mode 1 (Fig. 4a), and 9 compounds in the style of Mode 2 (Fig. 4b), as the lowest scored poses.

Site A was confirmed to be responsible for the PPIase activity of CypA and to serve as the binding site of the CA fragment of HIV and CsA, and thus several groups have made efforts to locate compounds that can fill this pocket as much as possible by screening and/or molecular design experiments [8, 21, 22]. Therefore, molecules that interact with CypA in Mode 1 were more likely to be investigated; however, the inhibitory activities of most of the candidates were limited to the micromolar level. To find potent inhibitor candidates with novel skeletons, we kept both Mode 1 and Mode 2 compounds for further biological evaluation.

Experimental results of viral replication and cell viability

Biological assays were performed to determine whether the 29 compounds and the 2 positive controls exerted inhibitory effects on viral replication and induced cellular toxicity. 293T cells were employed as virus-producing cells, whereas a T cell line, MT-4, and a reporter cell line expressing HIV-1 receptors, U87.CD4.CXCR4, were used as viral target cells. This assay system can evaluate the inhibitory effects of test compounds in a single replication cycle of HIV-1. The results demonstrated that most of the other tested compounds either did not exert noticeable inhibitory effects on HIV-1 replication or exhibited strong cytotoxicity at higher concentrations (Table 1). Moreover, although compound **4** exerted an inhibitory effect on viral replication, it displayed low solubility (Table 1); therefore, we did not evaluate this compound further. By contrast, two of our compounds, **12** and **23**, as well as the two positive control compounds, exerted potent inhibitory effects on HIV-1 replication while exhibiting low cytotoxicity at the effective concentration inhibiting viral growth by 50 % (Fig. 5). Compared with the control compounds **D4** and **FD8**, our hit compounds exhibited stronger inhibitory activities.

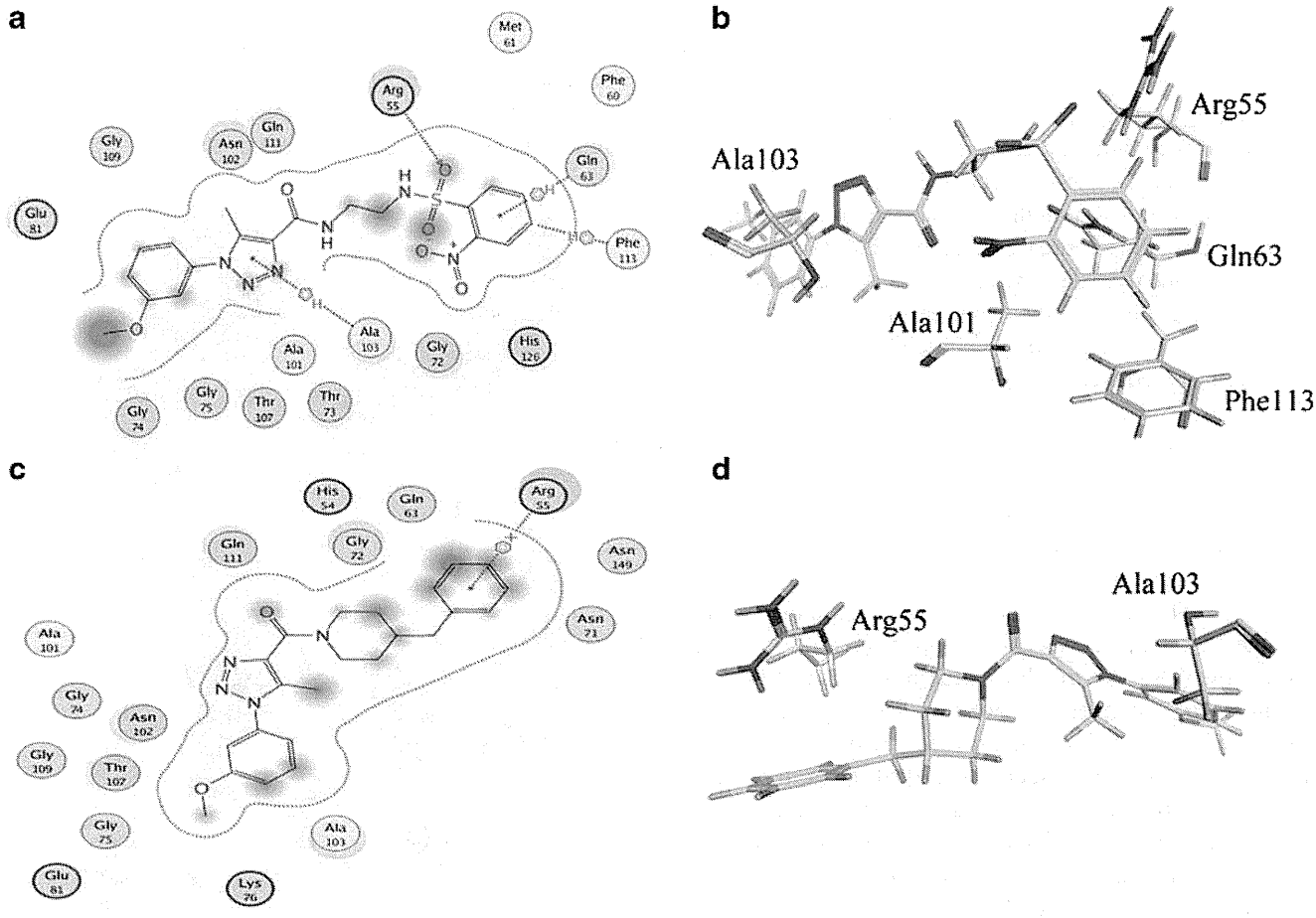

Fig. 7 Schematic view and docking pose of compound **23** (**a**, **b**) and compound **12** (**c**, **d**) with their binding sites. For docking poses, only important residues are displayed

Structural analysis of active compounds

The docking poses of compounds **23** and **12** were different. The best docking pose of **23** utilized Mode 1 binding (Fig. 6a), whereas that of **12** utilized Mode 2 binding (Fig. 6b). The interactions were first assessed using the Ligand Interactions module in MOE. These analyses provided direct schematic views of the interactions of **23** and **12** with CypA, as shown in Fig. 7a and c, respectively. Compound **23** inserted into both Site A and Site B. Figure 7a and b illustrate the dimensional interaction maps and docking poses, respectively, of **23** with CypA. The presence of 2-nitrobenzenesulfonamide appears responsible for the binding between **23** and Site A of CypA. The oxygen atom in the sulfonamide group interacts with the nitrogen atom at the ω position of Arg55 (**23**: O – CypA: Arg55: N^{ω}) within a distance of 2.9 Å. The aromatic ring of nitrobenzene interacts with both Gln63 and Phe113. Two edge-to-end (T-shaped) hydrogen-aromatic ring interactions (**23**:aromatic ring–CypA:Gln63:H and **23**:aromatic hydrogen–CypA:Phe113:aromatic ring) form a π–π stacking network. Because Arg55 and Phe113 are important pocket-forming residues and are highly conserved in most CypA isolates, these interactions are very meaningful for inhibitor design. Another key interaction revealed in the interaction map is the hydrophobic interaction between Ala103 and the triazole group of **23**. For **12**, arene-cation interactions (**12**: benzene ring–CypA: Arg55: NH1 and NH2) were detected. As mentioned above, Arg55 is a critical residue for ligand binding. These interactions can partly explain the activity of **12**.

Geometry-based interaction fingerprints provided loosely approximated insights into the fitting of our two active compounds into the receptor sites. However, it is difficult to determine the detailed intermolecular energies, particularly in terms of hydrophobic interactions. Therefore, we performed additional post-docking analyses. The interactions between binding site residues and active compounds were scrutinized using IF-E 6.0 [18] (created by Dr. Hooman Shadnia at Carleton University, http://www.shadnia.com/H_IFE/index.htm), retrievable from the SVL exchange service. This program can differentiate favorable ligand–residue interactions from unfavorable ones by force vectors and energy values. A negative sign indicates a stable interaction, whereas a positive sign indicates an unstable or repulsive interaction. The results of **23** and **12** for each residue near ligand atoms (less than 4.5 Å in distance) are

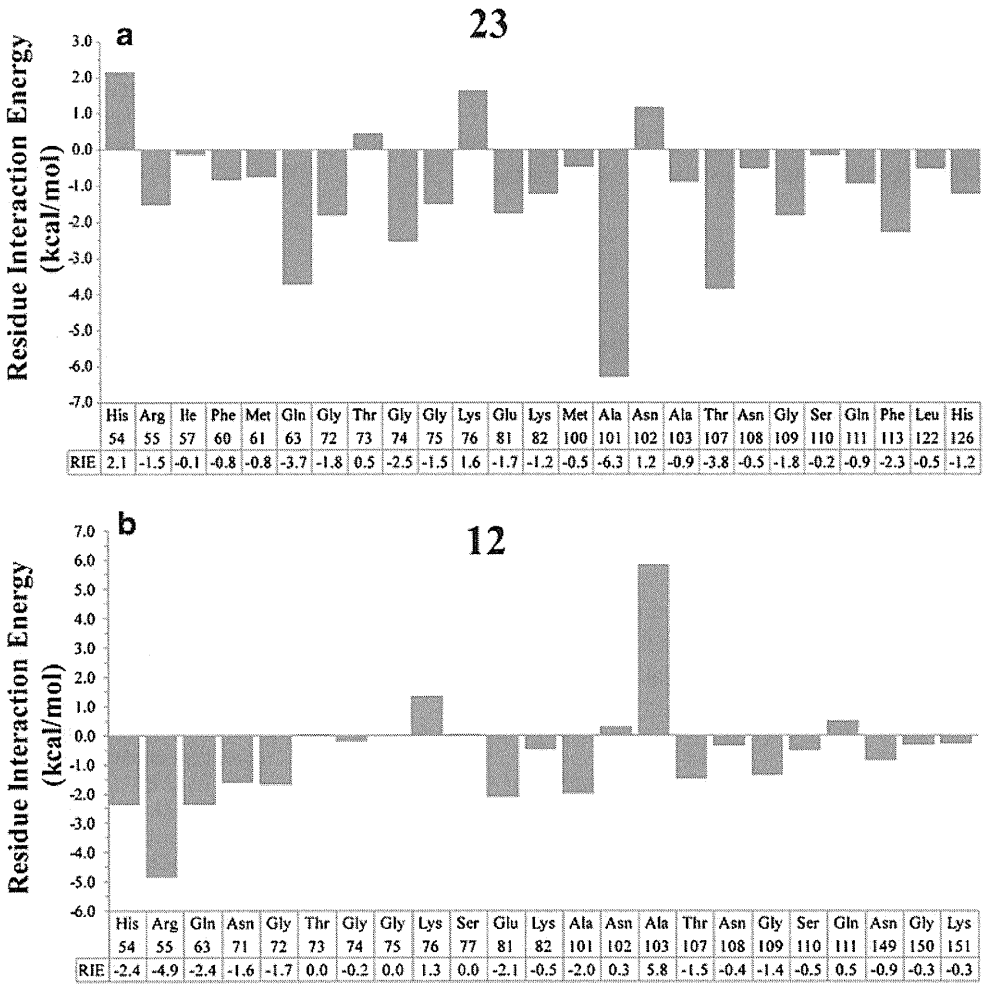

Fig. 8a,b Ligand–receptor interaction energy values (per-residue values) calculated using IF-E 6.0. The residue interaction energy data values are expressed in kcal mol^{-1}. **a** Graph for **23**, **b** graph for **12**

presented in Fig. 8. For **23**, in addition to the important residues mentioned above, we can see that Ala101 is also responsible for binding (Fig. 8a). The carbon in the Ala101 backbone is in approximation with the carbonyl oxygen of **23** (separated by 3.57 Å) (Fig. 7a). The dispersion force between the electron-poor environment of the Ala101 backbone carbon and the electron-rich environment of the carbonyl oxygen of **23** resulted in good binding effects. For **12**, the negative-signed interaction energy values, which indicate favorable residues for ligand binding, could be detected at multiple residues of CypA including the aforementioned residue Arg55. In addition to Arg55, other favorable residues for binding are listed in Fig. 8b. Conversely, a strong signal for a positive-signed peak could be detected at Ala103, suggesting that it is an unfavorable residue for the binding of **12**. By assessing atomic distances, we found that the methyl hydrogen atom of the Ala103 side chain and the aromatic hydrogen atom of **12** are approximately 1.8 Å apart (Fig. 7d). It can be concluded that the two hydrogen atoms clash with each other. However, it should be underlined that this docking pose was obtained from a rigid receptor docking procedure; therefore, this model cannot explain any "induced-fitting" phenomena. We assume that, due to the strong repulsion detected, the receptor residue should shift into a more appropriate orientation in a real system.

Compounds **23** and **12** have similar skeletons; however, they exhibited different docking modes. Molecules that target the combination region of the two modes can be assumed to be more active. These types of combined molecules are now under investigation using in-silico-based methods.

Conclusions

The present work involved the discovery of HIV-1 inhibitors targeting CypA via in silico and biological screening methods. Twenty-nine compounds selected from a database, together with control compounds, were examined for antiviral activities. Two of the compounds exhibited comparatively good effects in biological assays. In particular, compounds **12** and **23** both exhibited anti-HIV-1 activities with relatively low cytotoxicity at the effective concentration inhibiting viral growth by 50 %. From our experimental results, **12** and **23** may be used as lead compounds for novel type of anti-HIV inhibitors, although biochemical experiments to confirm that the target is really CypA are still needed.

Acknowledgments This study was supported by a Health Labor Sciences Research Grant, the Japanese Ministry of Health, Labor and Welfare, the program of the Japan Initiative for Global Research Network on Infectious Diseases (J-GRID) by the Ministry of Education, Cultures, Sports, Science and Technology (MEXT) of Japan, and Grants-in-Aid for the Systematic Graduate School Education Innovation Program (development of health and environment risk management experts) from MEXT of Japan.

References

1. Ke H, Huai Q (2003) Structures of calcineurin and its complexes with immunophilins-immunosuppressants. Biochem Biophys Res Commun 311:1095–1102
2. Foster TL, Gallay P, Stonehouse NJ, Harris M (2011) Cyclophilin A interacts with domain II of hepatitis C virus NS5A and stimulates RNA binding in an isomerase-dependent manner. J Virol 85:7460–7464
3. Chatterji U, Bobardt MD, Lim P, Gallay PA (2010) Cyclophilin A-independent recruitment of NS5A and NS5B into hepatitis C virus replication complexes. J Gen Virol 91:1189–1193
4. Chen Z, Mi L, Xu J, Yu J, Wang X, Jiang J, Xing J, Shang P, Qian A, Li Y, Shaw PX, Wang J, Duan S, Ding J, Fan C, Zhang Y, Yang Y, Yu X, Feng Q, Li B, Yao X, Zhang Z, Li L, Xue X, Zhu P (2005) Function of HAb18G/CD147 in invasion of host cells by severe acute respiratory syndrome coronavirus. J Infect Dis 191:755–760
5. Lin TY, Emerman M (2006) Cyclophilin A interacts with diverse lentiviral capsids. Retrovirology 3:70
6. Zenke G, Strittmatter U, Fuchs S, Quesniaux VF, Brinkmann V, Schuler W, Zurini M, Enz A, Billich A, Sanglier JJ, Fehr T (2001) Sanglifehrin A, a novel cyclophilin-binding compound showing immunosuppressive activity with a new mechanism of action. J Immunol 166:7165–7171
7. Li Q, Moutiez M, Charbonnier JB, Vaudry K, Menez A, Quemeneur E, Dugave C (2000) Design of a Gag pentapeptide analogue that binds human cyclophilin A more efficiently than the entire capsid protein: new insights for the development of novel anti-HIV-1 drugs. J Med Chem 43:1770–1779
8. Li J, Tan Z, Tang S, Hewlett I, Pang R, He M, He S, Tian B, Chen K, Yang M (2009) Discovery of dual inhibitors targeting both HIV-1 capsid and human cyclophilin A to inhibit the assembly and uncoating of the viral capsid. Bioorg Med Chem 17:3177–3188
9. Chen K, Tan Z, He M, Li J, Tang S, Hewlett I, Yu F, Jin Y, Yang M (2010) Structure-activity relationships (SAR) research of thiourea derivatives as dual inhibitors targeting both HIV-1 capsid and human cyclophilin A. Chem Biol Drug Des 76:25–33
10. Vajdos FF, Yoo S, Houseweart M, Sundquist WI, Hill CP (1997) Crystal structure of cyclophilin A complexed with a binding site peptide from the HIV-1 capsid protein. Protein Sci 6:2297–2307
11. Mikol V, Kallen J, Pflugl G, Walkinshaw MD (1993) X-ray structure of a monomeric cyclophilin A-cyclosporin A crystal complex at 2.1 A resolution. J Mol Biol 234:1119–1130
12. Zhao Y, Ke H (1996) Mechanistic implication of crystal structures of the cyclophilin-dipeptide complexes. Biochemistry 35:7362–7368
13. Lipinski CA, Lombardo F, Dominy BW, Feeney PJ (1997) Experimental and computational approaches to estimate solubility and permeability in drug discovery and development settings. Adv Drug Deliv Rev 23:3–25
14. Adachi A, Gendelman HE, Koenig S, Folks T, Willey R, Rabson A, Martin MA (1986) Production of acquired immunodeficiency syndrome-associated retrovirus in human and nonhuman cells transfected with an infectious molecular clone. J Virol 59:284–291
15. Tokunaga K, Greenberg ML, Morse MA, Cunning RI, Lyerly HK, Cullen BR (2001) Molecular basis for cell tropism of CXCR4-dependent human immunodeficiency virus type 1 isolates. J Virol 75:6776–6785
16. Fouchier RA, Meyer BE, Simon JH, Fischer U, Malim MH (1997) HIV-1 infection of non-dividing cells: evidence that the amino-terminal basic region of the viral matrix protein is important for Gag processing but not for post-entry nuclear import. EMBO J 16:4531–4539
17. Björndal A, Deng H, Jansson M, Fiore JR, Colognesi C, Karlsson A, Albert J, Scarlatti G, Littman DR, Fenyö EM (1997) Coreceptor

usage of primary human immunodeficiency virus type 1 isolates varies according to biological phenotype. J Virol 71:7478–7487
18. Shadnia H, Wright JS, Anderson JM (2009) Interaction force diagrams: new insight into ligand-receptor binding. J Comput Aided Mol Des 23:185–194
19. Dal Ben D, Buccioni M, Lambertucci C, Marucci G, Thomas A, Volpini R, Cristalli G (2010) Molecular modeling study on potent and selective adenosine A(3) receptor agonists. Bioorg Med Chem 18:7923–7930
20. Zydowsky LD, Etzkorn FA, Chang HY, Ferguson SB, Stolz LA, Ho SI, Walsh CT (1992) Active site mutants of human cyclophilin A separate peptidyl-prolyl isomerase activity from cyclosporin A binding and calcineurin inhibition. Protein Sci 1:1092–1099
21. Guichou JF, Viaud J, Mettling C, Subra G, Lin YL, Chavanieu A (2006) Structure-based design, synthesis, and biological evaluation of novel inhibitors of human cyclophilin A. J Med Chem 49:900–910
22. Chen S, Zhao X, Tan J, Lu H, Qi Z, Huang Q, Zeng X, Zhang M, Jiang S, Jiang H, Yu L (2007) Structure-based identification of small molecule compounds targeting cell cyclophilin A with anti-HIV-1 activity. Eur J Pharmacol 565:54–59

Original Paper

Intervirology

Intervirology
DOI: 10.1159/000339985

Received: August 8, 2011
Accepted after revision: June 4, 2012
Published online: ■■■

Chikungunya Virus Induces a More Moderate Cytopathic Effect in Mosquito Cells than in Mammalian Cells

Yong-Gang Li[a] Uamporn Siripanyaphinyo[b] Uranan Tumkosit[b]
Nitchakarn Noranate[b] Atchareeya A-nuegoonpipat[c] Ran Tao[a] Kurosu Takeshi[a]
Kazuyoshi Ikuta[a] Naokazu Takeda[b] Surapee Anantapreecha[c]

[a]Department of Virology, Research Institute for Microbial Diseases, Osaka University, Osaka, Japan; [b]Section of Viral Infections, Thailand-Japan Research Collaboration Center on Emerging and Re-Emerging Infections, and [c]National Institute of Health, Department of Medical Sciences, Ministry of Public Health, Nonthaburi, Thailand

Key Words
Chikungunya virus · Apoptosis · C6/36 cells · Vero cells · Cytopathic effect · Persistent infection

Abstract
Objectives: Chikungunya virus (CHIKV) is an alphavirus belonging to the Togaviridae family. Alphaviruses cause a chronic non-cytopathic infection in mosquito cells, while they develop a highly cytopathic infection in cells originating from various vertebrates. In this study, we compared the cytopathic effect (CPE) induced by CHIKV in Vero cells and a mosquito cell line, C6/36 cells. ***Methods:*** CPE and the virus titers were compared between the CHIKV-infected C6/36 and Vero cells. Apoptosis was measured by TUNEL assay, and the differences between the C6/36 and Vero cells were compared. ***Results:*** CHIKV infection induced strong CPE and apoptosis in the Vero cells, but light CPE in the C6/36 cells. The virus titers produced in the C6/36 cells were much higher than those produced in the Vero cells. ***Conclusions:*** The reason CHIKV induced strong CPE is that this virus triggers strong apoptosis in Vero cells compared with C6/36 cells. CHIKV established a persistent infection in C6/36 cells after being passaged 20 times. CHIKV infection in mosquito cells was distinct from that in Vero cells. The cell and species specificity of CHIKV-induced cell death implies that the cellular and viral regulators involved in apoptosis may play an important role in determining the outcome of CHIKV infection.

Introduction

Chikungunya virus (CHIKV), the causative agent of chikungunya fever, was first described in 1952 during an epidemic in Tanzania, East Africa [1]. CHIKV is a positive-sense single-strand RNA virus belonging to the genus *Alphavirus* in the family Togaviridae, and is maintained in two distinct transmission cycles, a sylvatic cycle and human-mosquito-human cycle. The scale of the epidemics for the former is smaller than the latter, and mainly confined within African countries involving primates, such as monkeys and forest-dwelling Aedes mosquitoes [2, 3]. The main vectors of CHIKV transmission in the human-mosquito-human cycle are *Aedes aegypti and Aedes albopictus*. Since its first outbreak in East Africa,

KARGER
Fax +41 61 306 12 34
E-Mail karger@karger.ch
www.karger.com

0300–5526/12/0000–0000$38.00/0

Accessible online at:
www.karger.com/int

Yong-Gang Li
Department of Virology
Research Institute for Microbial Diseases
Osaka University, Osaka (Japan)
Tel. +81 6 6879 8309, E-Mail yonggang@biken.osaka-u.ac.jp

CHIKV epidemics have often been characterized by long interepidemic periods of more than 10 years in many parts of Southern and Southeast Asia [4, 5]. During the past 8 years, the major outbreaks have occurred on islands in the Indian Ocean. Reunion Island has been among the most severely hit, with one third of its population infected and more than 240 deaths recorded [6]. The symptoms of chikungunya generally start 4–7 days after the bite, and the acute phase, lasting 1–10 days, is characterized by painful polyarthralgia, high fever, asthenia, headache, vomiting, rash, and myalgia [1, 7]. Chikungunya has affected as many as 3–4 million people in the Indian Ocean zone; it spread to Europe in 2005–2007, and recent outbreaks in Thailand have received considerable attention [8].

Both mosquito and vertebrate cell culture systems have been used to study CHIKV replication and pathogenesis [9]. Mosquito cells derived originally from *A. albopictus* larvae in particular have been employed in these studies. CHIKV is also able to infect a wide range of vertebrate cells and cell lines [10, 11], and most of these show an apparent cytopathic effect (CPE) [9]. A similar phenomenon was found in sindbis virus (SINV) infection, where almost all vertebrate cells died after infection, and the cell lines derived from mosquito are known to provide a long-term persistent infection [12]. The cell line derived from mosquito is known to provide a long-term persistent infection which is probably maintained by intracellular factors [13]. The viruses belonging to the alphavirus family have appeared to grow in cultured vertebrate and invertebrate cells [14]. Although alphaviruses cause encephalitis, neuronal apoptosis and death in mammals, they fail to kill the mosquitoes that can transmit these viruses. Therefore, host cell factors as well as viral factors regulate the outcome of the infection [15].

SINV is thought to cause a persistent infection in mosquito cells with moderate CPE in general [16]. We thought that CHIKV might also cause milder CPE in mosquito cells than in mammalian cells, and would lead to persistent infection in mosquito cells. The study on the pathogenicity of CHIKV is inadequate. Since Vero cells and C6/36 cells are commonly used in the propagation of flaviviruses such as dengue virus and togaviruses such as SINV [17–19], we used these two cells to study the pathogenesis of CHIKV infection. We found that CHIKV induced light CPE in mosquito cells, C6/36, but strong CPE in Vero cells. C6/36 produced higher titers of the progeny viruses compared to the Vero cells. CHIKV seems to establish a persistent infection in C6/36 cells when passaged 20 times. Interestingly, we also found that CHIKV induced stronger apoptosis in Vero cells than in C6/36 cells, although the mechanism is not yet known.

Materials and Methods

Virus and Cells

CHIKV Ross strain was propagated in Vero-E6 (Vero) cells which were maintained in MEM supplemented with 10% newborn calf serum and antibiotics at 37° in 5% CO_2. C6/36 cells were maintained in Leibovitz's L-15 Media (Invitrogen, Carlsbad, Calif., USA) supplemented with 10% newborn calf serum, antibiotics and 1% TPB (Sigma, St. Louis, Mo., USA) at 32°. All experiments were performed in a biosafety level 3 containment laboratory.

Immunofluorescence Assay

CHIKV- and mock-infected cells were fixed with 4% paraformaldehyde, and incubated 30 min at 37° with monoclonal antibody against the CHIKV E2 protein followed by FITC-conjugated anti-mouse IgG (Invitrogen) for 30 min at 37°. The monoclonal antibody was provided by Dr. P. Depres [20].

Plaque Assay

Vero cells were seeded at 1×10^6 cells per well in 6-well plates and incubated at 37° overnight. The cells were washed once with phosphate-buffered saline (PBS). Ten-fold serial dilutions of the virus were prepared in Hanks Buffer (Sigma-Aldrich), and 0.2 ml of the solution was inoculated into each well and incubated for 1 h at 37°. During incubation, the plates were gently agitated every 15 min. After the adsorption, the virus solution was removed and the cells washed three times with PBS. Two ml of 1% agrose in 2× MEM containing 0.5% FBS was layered onto the cell monolayers. The plates were incubated in a humidified incubator at 37° with 5% CO_2 for 3 days, and then the agarose overlay was removed and washed with PBS. The plaques were visualized by staining the monolayer with 2 ml of 0.25% crystal violet in 10% formaldehyde solution (Sigma-Aldrich) for 2 h at room temperature. The plates were washed and the plaques counted.

TUNEL Staining

The Vero and C6/36 cells (2×10^6) were infected at a multiplicity of infection (MOI) 1, and apoptotic cells were characterized by terminal deoxynucleotidyl transferase-mediated dUTP-biotin nick end labeling according to the manufacturer's instructions (DeadEnd Fluorometric TUNEL System; Promega). Briefly, after 24-hour postinfection (p.i.), the cells were fixed with 3% of paraformaldehyde in PBS containing 0.1% Triton X-100, washed with PBS three times, and incubated in a labeling reaction mixture containing terminal deoxynucleotidyl transferase enzyme, fluorescein isothiocyanate-conjugated nucleotide, and labeling buffer. The reaction was quenched in stop buffer, and the cells were washed with PBS several times. The cell nuclei were counterstained with propidium iodide (Sigma-Aldrich). Apoptosis was induced by a protein synthesis inhibitor, anisomycin, according to the manufacturer's instructions, and used as the positive control.